The Effects of Synaptic Noise on Measurements of Evoked Excitatory Postsynaptic Response Amplitudes

Linda M. Wahl,#* J. Julian B. Jack,# Alan U. Larkman,# and Kenneth J. Stratford#
#University Laboratory of Physiology, Parks Road, Oxford OX1 3PT, and *Mathematical Institute, Oxford OX1 3LB, England

ABSTRACT Spontaneously occurring synaptic events (synaptic noise) recorded intracellularly are usually assumed to be independent of evoked postsynaptic responses and to contaminate measures of postsynaptic response amplitude in a roughly Gaussian manner. Here we derive analytically the expected noise distribution for excitatory synaptic noise and investigate its effects on amplitude histograms. We propose that some fraction of this excitatory noise is initiated at the same release sites that contribute to the evoked synaptic event and develop an analytical model of the interaction between this fraction of the noise and the evoked postsynaptic response amplitude. Recording intracellularly with sharp microelectrodes in the in vitro hippocampal slice preparation, we find that excitatory synaptic noise accounts for up to 70% of the intracellular recording noise, when inhibition is blocked pharmacologically. Up to 20% of this noise shows a significant correlation with the evoked event amplitude, and the behavior of this component of the noise is consistent with a model which assumes that each release site experiences a refractory period of ~60 ms after release. In contrast with classical models of quantal variance, our models predict that excitatory synaptic noise can cause the apparent variance of successive peaks in an excitatory synaptic amplitude histogram to decrease from left to right, and in some cases to be less than the variance of the measured noise.

INTRODUCTION

The analysis of evoked postsynaptic responses can provide an important tool in addressing some fundamental questions about synaptic transmission in the central nervous system, such as the number of release sites at a given synaptic connection, the release probability at each site in response to an applied stimulus, or the size of the single quantal event (for reviews see Korn and Faber, 1987, 1991; Redman, 1990; Stevens, 1993). Frequency histograms of the peak amplitudes of synaptic events have been used to support both sides of contentious issues, such as the saturation of postsynaptic receptors (for example Jack et al., 1981; Bekkers et al., 1990; Kullmann, 1993), or the mechanism of long-term potentiation in the hippocampus, a long-lasting increase in synaptic strength that is thought to underlie learning and memory (Bekkers and Stevens, 1990; Malinow and Tsien, 1990; Foster and McNaughton, 1991; Malinow, 1991; Kullmann and Nicoll, 1992; Larkman et al., 1992; Liao et al., 1992; Voronin et al., 1992b; Stricker et al., 1996b).

Following the analytical protocol established at the neuromuscular junction (del Castillo and Katz, 1954; Boyd and Martin, 1956), the earliest analyses of synaptic amplitude histograms recorded in the central nervous system did not model background noise explicitly (for example Kuno, 1964). It soon became apparent, however, that amplitude histograms recorded in central neurons were better described by a model that incorporated the contribution of background noise (Edwards et al., 1976). Techniques for extracting information from synaptic amplitude histograms have since grown increasingly sophisticated, including numerous deconvolution methods (Wong and Redman, 1980; Jack et al., 1981; Ling and Tolhurst, 1983), expectation-maximization algorithms (Kullmann, 1989; Stricker and Redman, 1994), maximum entropy techniques (Kullmann, 1992), binomial approaches (Voronin et al., 1992a), the analysis of model moments (Dityatev et al., 1992), Bayesian statistical analysis (Turner and West, 1993), and statistical descriptions of response distributions over time (Blum and Idiart, 1994). Each of these techniques assumes that the background noise in the recording is independent of the evoked signal; in practice this background noise is generally modeled by a single Gaussian distribution or by the sum of two Gaussian functions (but see, for example, Kullmann, 1989).

One potential source of background noise in microelectrode recordings, however, is synaptic noise—synaptic events generated by spontaneously occurring action potentials or the spontaneous release of neurotransmitter at a synapse. The interaction between spontaneous and evoked release at the neuromuscular junction has been described by Barrett et al. (1974), and Korn and Faber (1990) present a detailed study of the structure and underlying quantal behavior of synaptic noise at a central inhibitory synapse. Although the effect of synaptic noise on measures of evoked synaptic amplitudes has not yet been modeled explicitly, Edwards et al. suggested as early as 1976 that fluctuations in the evoked response recorded in spinal motoneurons may be masked to a large degree by synaptic noise, and that synaptic noise may not be independent of the evoked event (see also Clamann et al., 1991; Solodkin et al., 1991).

The effect of a spontaneous synaptic event on the measurement of the peak amplitude of an evoked response

Received for publication 9 September 1996 and in final form 12 April 1997.
Address reprint requests to Dr. Kenneth J. Stratford, University Laboratory of Physiology, Parks Road, Oxford OX1 3PT, England. Tel.: 44-1865-272535 or 272500; Fax: 44-1865-272469; E-mail: kenneth.stratford@physiol.ox.ac.uk.

0006-3495/97/07/205/15 $2.00

amplitude will depend on the time interval between the spontaneous and evoked events. If the spontaneous and evoked events occur simultaneously, the measured amplitude of the evoked event will be increased by the amplitude of the spontaneous event. In contrast, if a spontaneous event reaches its peak height before the evoked event, the measured amplitude of the evoked event will be decreased, because the measurement will be made during the decay phase of the spontaneous event (see Soucek, 1971). If spontaneous synaptic events have short rise times and longer decay times, the probability that a spontaneous event will cause an increase in the measured amplitude will be much smaller than the probability of causing a decrease. It is therefore unlikely that the distribution of noise contributions from spontaneous synaptic events will be well approximated by a Gaussian function.

It is also possible that synaptic noise may not be independent of the evoked postsynaptic response, i.e., fluctuations in the evoked amplitude may be coupled in some way to fluctuations in the background noise. Although only a fraction of the release sites on a given cell may be stimulated during an experiment, this small subset of connections could be very active in producing spontaneous synaptic events. It is well known that at the neuromuscular junction, the probability of recording a miniature endplate potential is transiently increased after an evoked event, presumably because of high residual calcium concentrations in the axon terminal (del Castillo and Katz, 1954; Katz and Miledi, 1965; Rahamimoff and Yaari, 1973; Bornstein, 1978; Van der Kloot and Molgó, 1995). Similarly, increased synaptic noise has been observed after stimulation at central synapses (Manabe et al., 1992; Mennerick and Zorumski, 1995). If a substantial proportion of the synaptic noise is generated at release sites that are also involved in generating the evoked signal, signal and noise will not be independent.

The effects of synaptic noise may be related to two puzzling observations reported by several laboratories working with excitatory inputs to CA1 pyramidal cells in the hippocampus. First, the peaks of some histograms of evoked synaptic amplitudes are better fitted by using distributions with variance less than the variance of the contaminating noise measured in the baseline period (Larkman et al., 1991; Liao et al., 1992; Voronin et al., 1992a; Stricker et al., 1996b). Second, some histograms appear to show zero or very low levels of quantal variance. Variance in the amplitude of single quantal responses will lead to the variance of evoked responses increasing with the number of quanta they contain. Thus the peaks in evoked amplitude histograms would be expected to become broader and less clear from left to right, and this effect has been clearly demonstrated at the vertebrate neuromuscular junction (e.g., Boyd and Martin, 1956). However, some histograms from hippocampal synapses show no apparent increase in variance with increasing numbers of quanta (Larkman et al., 1991; Liao et al., 1992; Voronin et al., 1992a; Stricker et al., 1996a), and in some cases are best fit by sums of Gaussian distributions whose variance actually decreases from small to large amplitudes (Stratford et al., 1994). The level of quantal variance at hippocampal excitatory synapses is a controversial issue (e.g., Bekkers and Stevens, 1995), but given the stochastic opening of postsynaptic channels, it is unlikely to be zero. Finite sampling invariably complicates the interpretation of experimental histograms and could be at least a partial explanation for these phenomena. A further possibility arises from the different kinds of contribution that intersite quantal variance makes to such histograms (Wahl et al., 1995). Nevertheless, we felt it was worth exploring whether there were circumstances under which synaptic noise could contribute to such effects.

In this paper we derive an analytical model for the effects of synaptic noise on measures of evoked postsynaptic amplitudes. The model indicates that, provided synaptic noise constitutes a significant proportion of the total recording noise, the positions and shapes of histogram peaks will be affected. With high levels of synaptic noise, peak width can decrease with higher peak number. We go on to consider the case in which some of the synaptic noise is generated at the same release sites involved in the evoked synaptic event. If there is some refractoriness after release, the synaptic noise and evoked signal will not be independent, and the best fit variance to one or more peaks in the amplitude histogram can be lower than the background noise. To see if these model predictions are likely to be relevant to experimental situations, we went on to perform simple experiments in hippocampal slices to estimate the proportion of the total noise that is of synaptic origin, and whether some component of this shows interdependence with the evoked signal. These experiments suggest that a substantial component of the noise is synaptic, and that a proportion of this is indeed dependent on the evoked synaptic amplitude. Thus the effects highlighted by our model are likely to influence experimental results, at least under the conditions we have used.

ANALYTICAL MODELING

A model of background synaptic noise

In this section we examine the effect of a single spontaneous synaptic event on the measured amplitude of the evoked event. We then combine this with a Poisson model for the arrival times of spontaneous synaptic events to determine the distribution of noise contributed by spontaneous events occurring at a given frequency.

The noise amplitude distribution for a single spontaneous event

The peak amplitude of a synaptic event is typically measured by subtracting the average voltages recorded during two short windows of the trace (Fig. 1 *A*); the separation between these windows is determined by the latency and the rise time, τ, of the event. If the latency is short, evoked amplitudes are thus measured by subtracting the voltage

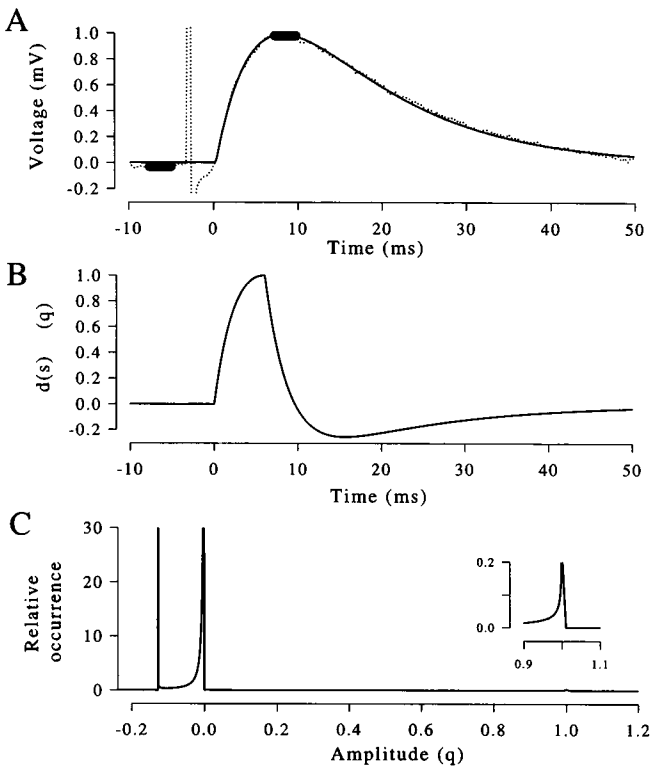

FIGURE 1 The synaptic noise amplitude distribution. (*A*) The average of 100 consecutive EPSPs evoked in a hippocampal pyramidal cell is plotted (*dotted line*). The extracellular stimulus was applied at time 0. The amplitude of the EPSP is measured by subtracting the average voltage recorded during the two 2.5-ms time windows marked by dark bars immediately before the stimulus and at the peak of the EPSP. For this example, the peak height of the average trace is 1.03 mV, the time to peak is 6.0 ms, and the 10–90% rise time is 4.5 ms. The solid line shows the best fit to this average EPSP obtained for the difference between two exponential functions, given by $h(t) = 1.88(e^{-65.2t} - e^{-339.9t})$, where h is the voltage in millivolts and t is the time in seconds. (*B*) Time course of the difference function. For the synaptic event shown in *A*, the simulated voltage at each time has been subtracted from the voltage τ seconds later, where τ is the rise time of the synaptic event: $d(s) = h(t) - h(t - \tau)$. (*C*) The expected contribution of synaptic noise to the measured amplitude for a single spontaneous event occurring within 100 ms before the evoked event. The probability density function is plotted against the amplitude of the noise contribution. The peak at the origin and the subpeak to the left of the origin have been truncated; the latter peak demonstrates the high probability that the amplitude measurement window occurs early on the falling phase of the spontaneous event (see text). Note the small peak on the extreme right, corresponding to the probability that the spontaneous event nearly coincides with the measurement windows. The inset shows this peak in greater detail; axis units are the same as those used in the main graph.

recorded at one time from the voltage recorded about one event rise time later. The error in this measurement caused by a spontaneous synaptic event depends on when the spontaneous event occurs relative to the evoked event.

Suppose that spontaneous synaptic events have the same general shape as an evoked postsynaptic response. Fig. 1 *B* shows the difference function, the voltage at each time subtracted from the voltage recorded one rise time later, for the time course of the synaptic event, $h(t)$, shown in Fig. 1 *A*. The difference function is given by $d(s) = h(s) - h(s - \tau)$. If the amplitude of an evoked event is measured at a fixed point in a recording, and the only contribution to the background noise is a spontaneous synaptic event that occurs at some time before the evoked amplitude measurement, this function shows the effect of the spontaneous event on the measured amplitude. Thus if the spontaneous event occurs nearly simultaneously with the evoked event, the measure of the evoked amplitude will be increased by one quantal unit. As described previously, it is more likely that the measured amplitude will be decreased, because the measurement is being made during the falling phase of a contaminating spontaneous event.

Let $u(s)$ be the probability density function of s; $u(s)$ represents the probability that the spontaneous event will occur s seconds before the peak of the evoked event, given that one and only one event occurs. If spontaneous events occur randomly and are Poisson-distributed, then the probability of an event occurring at every time is the same; $u(s)$ is uniform. The probability of contributing a given amount, a, to the amplitude measurement is then given by the theorem for the transformation of a random variable (see, for example, Papoulis, 1991, p. 93): if $a = d(s)$ is a function of a random variable s, and s has a probability density function, $u(s)$, then the probability density function for a is

$$b_1(a) = \sum_{i=1}^{n_r} \frac{u(s_i)}{|d'(s_i)|} \tag{1}$$

where $d'(s)$ is the first derivative of $d(s)$ with respect to s, and the s_i (for $i = 1$ to n_r) are the real roots of the equation $a = d(s)$.

Fig. 1 *C* shows this expected noise contribution, $b_1(a)$, for the synaptic waveform shown in Fig. 1 *A*. For simplicity, we assume that a spontaneous event that is initiated at s decays to zero amplitude by time $s + T$, and therefore define the probability density function of s, $u(s)$, to be $1/T$ for all s between 0 and T. The s_i were determined numerically using Brent's method (Press et al., 1988).

The probability density function shown in Fig. 1 *C* indicates that a single spontaneous event that occurs at some random time before an evoked event will contribute near-zero amplitude to the measurement of an evoked event with a very high probability (the peak at zero has been truncated in the figure). A second peak in the distribution, however, occurs to the left of the origin, indicating a relatively high probability that the measurement of the evoked event will occur on the early falling phase of the spontaneous event. A very small peak also occurs at the amplitude of the spontaneous event, q; this peak represents the small probability that the spontaneous event will occur nearly simultaneously with the evoked event.

Noise amplitude distribution for events at a given frequency

If more than one miniature spontaneous event occurs before the evoked event, what is the expected noise contribution to

the measured amplitude? The probability density function of the sum of two random variables is given by the convolution of their probability density functions. If we assume that distinct synaptic events add linearly, then the convolution of $b_1(a)$ with itself will give the expected distribution if two spontaneous events occur at random times before the evoked event; $b_2(a) = b_1(a)*b_1(a)$ (where * denotes convolution), and in general, $b_i(a) = b_{i-1}(a)*b_1(a)$. If no spontaneous event occurs before the evoked event, the noise contribution will be zero; $b_0(a)$ is a delta function at the origin.

Although the intervals between spontaneous synaptic events in the peripheral nervous system are not well described by a Poisson process (Cohen et al., 1974; Bornstein, 1978), the Poisson model does describe the timing of spontaneous miniature events in some central synapses (for example, Auerbach, 1971; Brown et al., 1979; but see Korn and Faber, 1990). If spontaneous synaptic events are Poisson-distributed with mean frequency F, the probability of exactly j events occurring in time interval T is given by $e^{-FT}(FT)^j/j!$. Suppose that the background spontaneous event frequency is 10 Hz and T is 50 ms. No spontaneous events would occur within T ms of the evoked event 61% of the time; one event would occur 30% of the time; and two events would occur 8% of the time. To predict the overall probability density function for the background noise, 61% of $b_0(a)$ can be added to 30% of $b_1(a)$ and 8% of $b_2(a)$. This process is illustrated in Fig. 2. Note the appearance of gradually diminishing subpeaks to the left of the origin in the overall noise distribution (Fig. 2 *D*); these correspond to situations in which one or two spontaneous events occur before the noise measurement, that is, the measurement is made during the falling phase of one or two events.

The dotted line in Fig. 2 *D* shows the noise distribution smoothed by a digital Gaussian filter (SD 0.1 q). We use this smoothing technique simply to help visualize the overall effects of the synaptic noise, which are difficult to evaluate from the distribution of subpeaks. We try to use the minimum smoothing factor that will join the individual subpeaks; for consistency, we have used 0.1 q throughout the paper.

The smoothed noise distribution for synaptic noise at frequencies between 0 and 50 Hz is illustrated in Fig. 3 *A*. Note that, as in the distribution shown in Fig. 2 *D*, peaks are shifted to the left and slightly skewed. The negative shift is more pronounced at higher spontaneous event frequencies; at these frequencies a very small peak also appears to the right of the origin. Table 1 gives the mean and SD of the best-fit Gaussian function for each of the distributions illustrated in Fig. 3 *A*; the best fit was obtained using commercially available software (Peakfit, Jandel Scientific).

We also investigated the effects of variations in both the peak amplitude (single or double (skewed) Gaussian distributions) and shape of the miniature responses comprising the synaptic noise. We found that whereas the small peak on the right of the noise distribution disappears for very small variations in size or shape, the negative skewness and shift

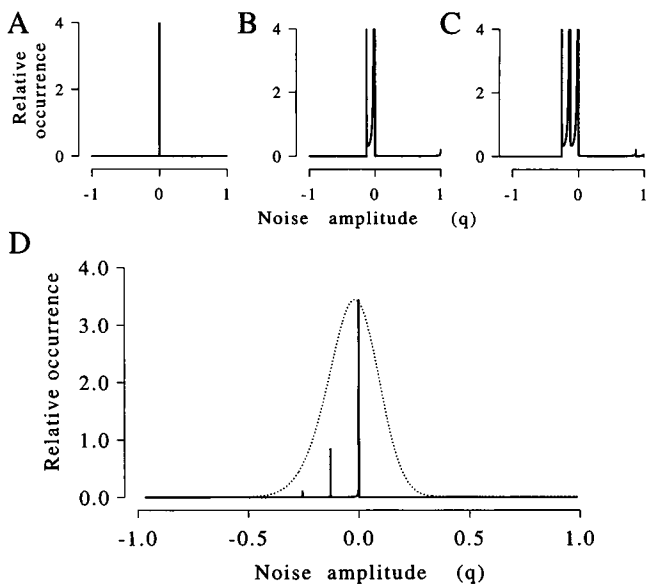

FIGURE 2 The distribution of noise from spontaneous events at 10 Hz. The expected noise contributions for zero, one, or two spontaneous events occurring before the amplitude measurement windows are shown in *A*, *B*, and *C*, respectively. The synaptic event waveform is shown in Fig. 1 *A*; synaptic events are assumed to decay to zero amplitude in 2 membrane time constants. Peaks have been truncated in these panels. (*D*) The solid line shows the sum of 60% of the curve shown in *A*, 31% of *B*, and 8% of *C*. This is the distribution of the noise expected for spontaneous events occurring at a frequency of 10 Hz, as described in the text. Note the subpeaks to the left of the origin. The dotted line shows the same distribution, smoothed by a Gaussian filter (SD 0.1 q) and scaled (by 6500) to the same peak height.

in the central peak are retained for spontaneous event amplitudes with a CV of 30% or more. Fig. 3 *B* illustrates these results for a single Gaussian distribution of miniature amplitudes with CVs between 0 and 50%.

Effects on amplitude histograms

Because of the underlying structure of synaptic noise, its effects on amplitude histograms are complex. Suppose each of three identical, independent release sites has a probability of 0.5 of contributing amplitude q to an evoked EPSP; the amplitude histogram predicted by simple binomial theory is shown in Fig. 4 *A*. To determine the effects of synaptic noise during the measurement of these amplitudes, this histogram can be convolved with the noise distribution derived by the methods presented in the previous section. Fig. 4 *B* shows this result for a spontaneous event frequency of 50 Hz. The dotted line shows the unsmoothed distribution, which includes numerous subpeaks to the left of each quantal peak. The solid line shows the same distribution smoothed by a Gaussian filter. Note that the peak positions have been shifted to the left by about a third of the quantal size; the first peak (no release) now has a negative amplitude, and each peak is no longer symmetrical. To the extreme right of the graph, an additional fourth peak is begin-

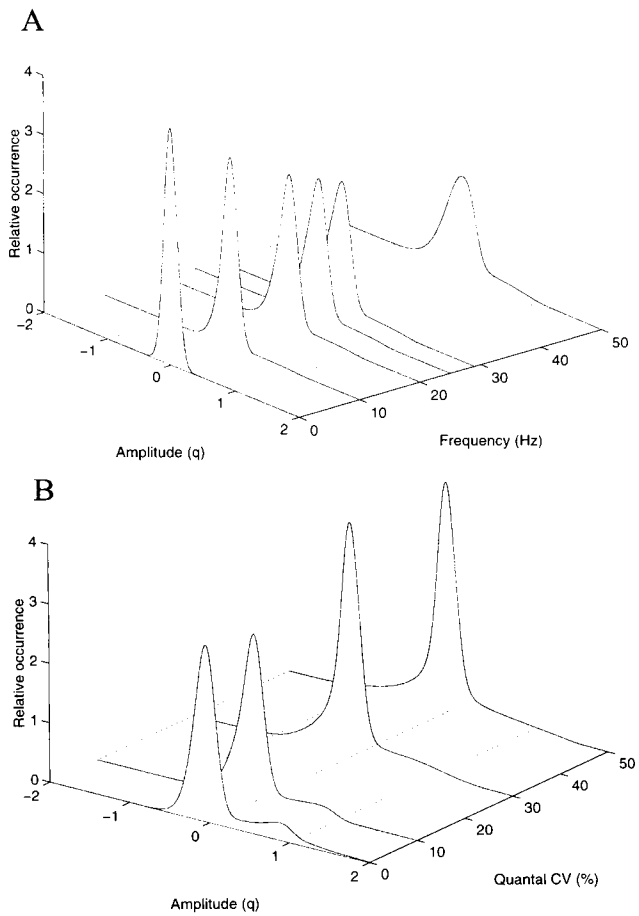

FIGURE 3 Noise contributions for spontaneous events at various frequencies and amplitudes. (*A*) Expected noise distributions for synaptic noise are plotted against the frequency of spontaneous events. Each synaptic event has a peak amplitude of one (Fig. 1 *A*) and is assumed to decay to zero amplitude in 100 ms. Frequencies between 0 and 50 Hz are shown. Note the broadening of the central peak and the increased skewness and shift to the left at high frequencies. A small peak to the right of the origin is visible at high frequencies. (*B*) Expected noise distributions for synaptic noise are plotted against the coefficient of variation (CV) of the peak amplitude of the single quantal event. In this example, the probability that each synaptic event has a given amplitude was modeled as a Gaussian distribution with mean 1.0 *q*. The event frequency was 25 Hz. To accentuate the small peak to the right of the origin, only synaptic events that occurred within 50 ms before the applied stimulus were considered in this model; note that this peak disappears if the CV of the single-event amplitude is ~30% or more.

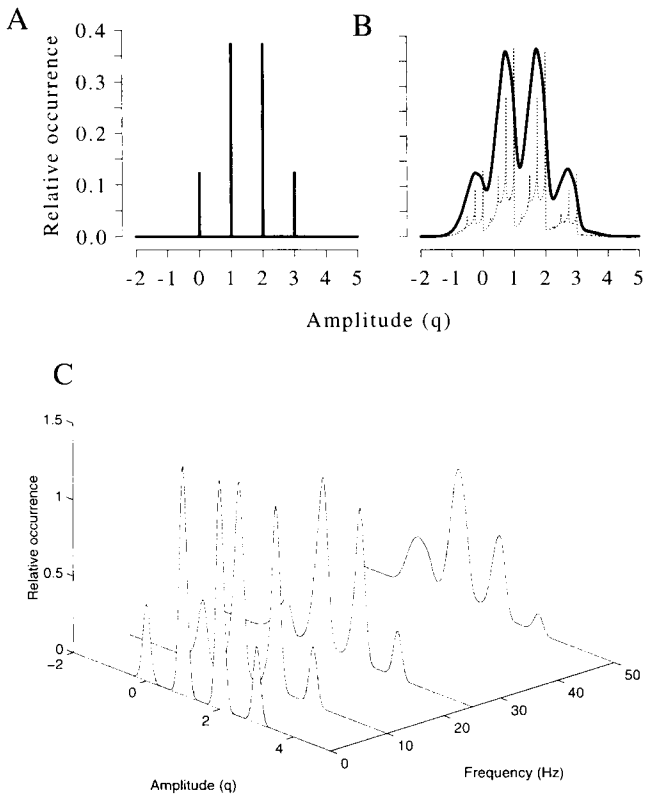

FIGURE 4 Effects of synaptic noise on an amplitude histogram. (*A*) The amplitude histogram predicted by a simple binomial model, for three release sites with a release probability of 0.5 and a quantal size of 1.0. (*B*) The dotted line shows the same histogram, convolved with the expected noise distribution for synaptic noise at 50 Hz. The events contributing to the synaptic noise have a double exponential waveform (Fig. 1 *A*), scaled to unit amplitude. Numerous subpeaks occur to the left of each peak; these peaks correspond to the probability that the amplitude of the evoked event is measured early on the falling phase of one or more spontaneous events. The solid line shows the same distribution, smoothed by a Gaussian filter with a SD of 0.1 *q*, and scaled (by 4.1) to the same peak height. The peak positions have been shifted to the left, and each peak is no longer symmetrical. (*C*) Effects on an amplitude histogram of synaptic noise at various frequencies. Amplitude histograms were derived as in *B*, but the frequency of spontaneous events was varied to 10, 25, and 50 Hz. The peaks are broadened and shifted increasingly to the left at higher frequencies (see Table 2 for estimates of peak position and SD).

ning to appear (although it is shifted to 3.5 or 3.7 *q*); this peak is caused by spontaneous events that occur nearly simultaneously with three evoked quanta.

TABLE 1 Mean and SD of synaptic noise distributions at various frequencies

Frequency (Hz)	10	20	25	29*	50
Mean (*q*)	−0.03	−0.08	−0.10	−0.12	−0.22
SD (*q*)	0.122	0.151	0.164	0.176	0.234

*Chosen for comparison with experimental results presented in this paper.

The effects of various frequencies of synaptic noise on the theoretical amplitude histogram shown in Fig. 4 *A* are shown in Fig. 4 *C*. From this figure it is clear that even low rates of synaptic noise can affect the positions and shapes of the peaks in an amplitude histogram. To investigate these effects more thoroughly, histograms such as those illustrated in this figure were fitted by a sum of four Gaussian functions; the means and SD of the best-fit Gaussian functions are shown in Table 2. Because the quantal size, *q*, is equal to 1, the coefficient of variation (CV, SD divided by mean) of each distribution is equal to its SD. Note that higher rates of synaptic noise shift the peak positions more toward the left, while increasing the peak widths. Also note that for synaptic noise at frequencies higher than 25 Hz, the peak widths decrease with higher peak number. Further-

TABLE 2 Positions and SD of peaks in amplitude histograms with synaptic noise

Frequency	Peak 0	Peak 1	Peak 2	Peak 3
0 Hz				
Mean (q)	0.00	1.00	2.00	3.00
SD (q)	0.100	0.100	0.100	0.100
10 Hz				
Mean (q)	−0.04	0.96	1.96	2.96
SD (q)	0.133	0.133	0.133	0.135
25 Hz				
Mean (q)	−0.05	0.95	1.95	2.94
SD (q)	0.229	0.204	0.201	0.202
30 Hz				
Mean (q)	−0.14	0.84	1.83	2.82
SD (q)	0.257	0.223	0.218	0.216
40 Hz				
Mean (q)	−0.19	0.79	1.77	2.76
SD (q)	0.301	0.254	0.246	0.238
50 Hz				
Mean (q)	−0.23	0.74	1.72	2.71
SD (q)	0.335	0.277	0.267	0.257

more, the peak heights (and areas, even more so) are relatively changed; those with higher quantal content are more reduced. This has the consequence that the deduced probability of release will be underestimated.

Synaptic noise from stimulated release sites

In this section we assume that some fraction of the synaptic noise is initiated at the same release sites that contribute to the evoked event, and that these release sites experience a brief refractory period after release (Stevens and Tsujimoto, 1995; Stevens and Wang, 1995). Because of this refractoriness, a release site that has just contributed some "noise" to the recording by producing a spontaneous event is less likely to contribute to the evoked signal when the stimulus is applied. Here we derive the time course of "correlated" noise, the component of synaptic noise that is dependent on the evoked signal. We then investigate the effects of this noise component on synaptic amplitude histograms.

An analytical model of correlations between signal and noise

We begin by deriving the probability that a single spontaneous event occurred at time t before the applied stimulus, assuming that we know the state of the release site, refractory or nonrefractory, at the time of the stimulus.

Suppose that a single release site produces spontaneous single quantal events according to a Poisson model with probability f per unit time. The probability of producing zero such events in time Δt is then $e^{-f\Delta t}$, and the probability of producing one or more is $1 - e^{-f\Delta t}$. For simplicity, we assume that after such an event is produced, the release site becomes refractory for a short time interval R, and then reverts to its original state instantaneously. Note that on average, the time spent waiting for an event to occur is f^{-1}; because the time spent in the refractory period is R, the overall frequency of spontaneous events, α, is $1/(R + f^{-1})$. The probability that the release site is refractory at any given time is $R/(R + f^{-1})$, and the probability that it is not in the refractory state is $f^{-1}/(R + f^{-1})$ or $1/(fR + 1)$.

At time $t = 0$, the stimulus is applied. What is the probability, $p(t|r)$, that a spontaneous event was produced at time t before the stimulus, given that the site is in a refractory state at $t = 0$? If the site was refractory when the stimulus was applied, then a spontaneous event must have occurred at some time between $t = -R$ and $t = 0$. Because the occurrence of the event at any time in this interval is equally likely, $p(t|r)$ equals $1/R$ for t in the interval $(-R, 0)$.

For t in the interval $(-2R, -R)$, the derivation is slightly more involved. The probability that a spontaneous event occurs at time $-R - \tau$ (or, more precisely, in the interval between $-R - \tau - \delta\tau$ and $-R - \tau$) is given by the expression $1 - e^{-\alpha\delta\tau}$. If this occurs, the site will be refractory until $-\tau$. For the site to be refractory at zero, a second event must occur in the interval $(-\tau, 0)$; the probability of an event occurring in this interval is given by $1 - e^{-f\tau}$. We can integrate for values of τ between 0 and t to obtain the cumulative probability that an event occurred in the interval $(t, -R)$ and that the site is refractory at $t = 0$, $P(t \cap r)$:

$$P(t \cap r) = \int_{\tau=0}^{t} (1 - e^{-\alpha\delta\tau})(1 - e^{-f\tau}) = \int_{\tau=0}^{t} \alpha(1 - e^{-f\tau})\delta\tau \tag{2}$$

Dividing by the probability that the site is refractory at $t = 0$ we find the cumulative probability, $P(t|r)$:

$$P(t|r) = \frac{\int_{\tau=0}^{t}\alpha(1 - e^{-f\tau})\delta\tau}{fR/(fR + 1)} \tag{3}$$

and differentiating, we find the probability density function, $p(t|r)$:

$$p(t|r) = \frac{1 - e^{-ft}}{R}, \quad \text{for } t \text{ in } (-2R, -R) \tag{4}$$

For t in the interval $(-3R, -2R)$, we derive probabilities as illustrated above, yielding

$$p(t|r) = \frac{1}{R}(ft + 2e^{-ft} - e^{-f(t+R)} - 1), \quad \text{for } t \text{ in } (-3R, -2R) \tag{5}$$

The first panel in Fig. 5 plots $p(t|r)$ for t between $-3R$ and zero, for $R = 50$ ms, $f = 16.67\ s^{-1}$. Intuitively, this function reflects the number of spontaneous synaptic events expected to occur at each time before an applied stimulus, given that the release site is in a refractory state at the time of the stimulus.

The probability that a spontaneous event occurred at time t, given that the site is nonrefractory at $t = 0$, $p(t|\text{non-}r)$, can be similarly derived. In exact analogy to the case for $p(t|r)$

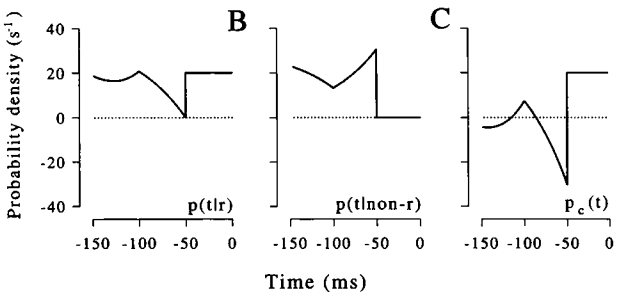

FIGURE 5 Analytical model of correlated noise. Solutions to the equations describing the correlated noise process are presented for a model with a refractory period, R, of 50 ms, and a probability of spontaneous events, f, of 16.67 s^{-1}. The probability of a spontaneous event occurring at time t, given that the release site is refractory at zero (A) or nonrefractory at zero (B), is shown. The difference between these two curves is plotted in C.

detailed above, we find that $p(t|\text{non-}r) = 0$ for t in $(-R, 0)$, and

$$P(t|\text{non} - r) = \frac{\int_{\tau=0}^{t} \alpha(e^{-f\tau})\delta\tau}{1/(fR + 1)}, \quad \text{for } t \text{ in } (-2R, -R)$$
$$p(t|\text{non} - r) = fe^{-ft} \tag{6}$$

Similarly:

$$p(t|\text{non} - r) = f(1 - e^{-ft} + e^{-f(t+R)}), \quad \text{for } t \text{ in } (-3R, -2R) \tag{7}$$

Fig. 5 B plots $p(t|\text{non-}r)$ for t between $-3R$ and zero. As in the previous case, this function reflects the number of spontaneous events expected to occur at each time before an applied stimulus, for a release site that is nonrefractory at the time of the stimulus. Fig. 5 C shows the difference between $p(t|r)$ and $p(t|\text{non-}r)$; the notation $p_c(t)$ has been introduced to describe this difference, which we refer to as the "correlated" noise probability distribution. Because the number of release sites that are in a refractory state at the time of the stimulus should be reflected in the trial-to-trial differences in the amplitude of the evoked event, we expect these functions to describe a component of the background noise that is correlated with evoked event amplitude. The application of these equations to experimental data is demonstrated later in this paper.

The Appendix provides an extension of this derivation in which the variance of the noise is predicted from the spontaneous event probabilities shown in Fig. 5.

Effects of synaptic noise from the stimulated release sites on amplitude histograms

We determined the effects of background synaptic noise on amplitude histograms by deriving the noise distribution produced by spontaneous synaptic events and convolving the theoretical amplitude histogram with this distribution. For synaptic noise initiated at the stimulated release sites, however, the interactions between signal and noise are slightly more complex.

If a spontaneous event occurs at a release site within one refractory period before the stimulus, that site will be refractory and will not contribute a quantum to the evoked event. Recall, however, that each release site contributes to the evoked event stochastically, on only a proportion of the trials. Spontaneous events that occur within R seconds of the stimulus can therefore be classified into two distinct groups: those that have no real effect on the number of quanta in the evoked event (occurring at release sites that would not have released on that trial), and those that effectively reduce the number of evoked quanta by one. Both classes of event will contribute some noise amplitude to the measured signal, as shown in Fig. 1 C. If a spontaneous event makes some noise contribution and reduces the measured amplitude by 1.0 q, the expected noise distribution would be the same as that pictured in Fig. 1 C, but shifted to the left by one quantal size (q). We can denote this distribution as $b_1(a + q)$.

The expected noise distribution caused by several spontaneous events at the stimulated sites can be determined by convolving appropriate combinations of $b_1(a)$ and $b_1(a + q)$. If j spontaneous events occur within R ms of the stimulus, and the evoked event is therefore reduced by l quanta, the probability density function of the noise, $c_{j,l}(a)$, is

$$c_{j,l}(a) = b_{j-l}(a) * b_l(a + q) \tag{8}$$

where $b_l(a + q)$ is simply $b_1(a + q)$ convolved with itself l times.

The probabilities of occurrence for values of j and l can be determined by multiplying the appropriate probabilities; we find that for n release sites and the kth peak of the histogram, the probability that the evoked quantal event is reduced by l quanta if j spontaneous events occur is given by

$$p(j, k, l, n) = \frac{(n - j)!\,(n - k)!\,k!\,j!}{n!\,(n - k - j + l)!\,(k - l)!\,l!\,(j - l)!} \tag{9}$$

From Poisson statistics, the probability that exactly j spontaneous events occur within R ms of the stimulus is given by $P(j) = e^{-\alpha R}(\alpha R)^j/j!$. The overall contribution of synaptic noise initiated at the stimulated release sites within R ms of the stimulus can therefore be calculated for peak k of the histogram as

$$C_k(a) = \sum_{j=0}^{n} P(j) \sum_{l=0}^{j} p(j, k, l, n) \cdot c_{j,l}(a) \tag{10}$$

Fig. 6 shows the amplitude histograms resulting from a three release site model, with a probability of release in response to the stimulus, for nonrefractory sites, of 0.5. The only noise process in the model is synaptic noise from the stimulated release sites. In the first panel, the refractory period is 30 ms, and the average frequency of spontaneous firing at the stimulated sites (including time spent in the refractory period) is varied between 0 and 50 Hz. In the

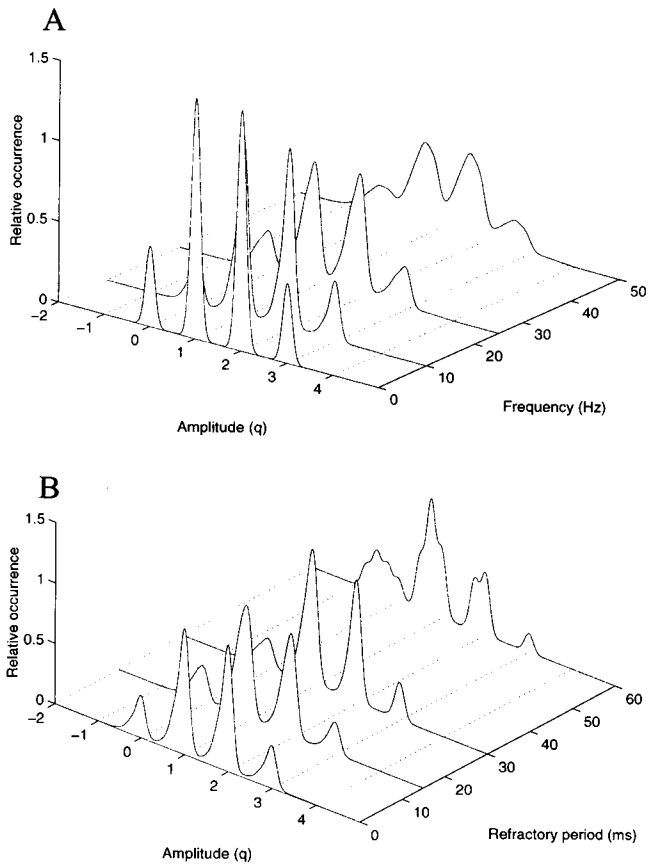

FIGURE 6 Effects of synaptic noise from the simulated release sites on an amplitude histogram. Amplitude histograms predicted by a simple binomial model, for three release sites with a release probability of 0.5 and a quantal size of 1.0, have been convolved with the expected noise distribution for synaptic noise from the stimulated release sites. Each peak of the histogram was convolved separately with the expected noise distribution for that peak, as described in Eq. 10, and the results were summed. The events contributing to the synaptic noise, and to the evoked event, have a double-exponential waveform (Fig. 1 *A*), scaled to unit amplitude. (*A*) The refractory period is 30 ms and the average frequency of spontaneous events from the stimulated sites (including time spent in the refractory period) is set to 0, 10, 25, and 50 Hz. (*B*) The average spontaneous event frequency was kept constant (25 Hz), and the refractory period varied between 0 and 60 ms. In both cases peaks on the left-hand side of the histogram are broadened and shifted to the left; also note the changes in relative peak height for high frequencies or long refractory periods (Table 3 gives estimates of peak position and SD). For a refractory period of 60 ms, the subpeaks in the distribution become prominent.

second panel, the average frequency of spontaneous firing is kept constant (25 Hz), and the refractory period is varied between 0 and 60 ms. The contribution of synaptic noise initiated at the stimulated release sites between R and T ms before the stimulus has also been included in these histograms (T = 100 ms); this component of the noise can simply be modeled as background synaptic activity, as derived in Eq. 1.

Note that peaks are broadened and shifted to the left in all cases, and that peak heights are markedly reduced at higher frequencies or for longer refractory periods. It is also interesting to note the relative change in peak heights—peaks with a higher quantal content are more likely to be reduced by spontaneous activity, and so the apparent probability of release is reduced. These effects are similar to those found for background synaptic noise from unstimulated release sites.

Table 3 gives the means and SD for the sums of Gaussians that best fit these histograms. It is interesting to note that in both *A* and *B*, the SD of successive peaks shows an overall tendency to decrease from left to right; this effect is greater for higher frequencies or longer refractory periods. The rightmost column of the table shows the SD of the background noise that would be expected (from Table 1) for spontaneous synaptic noise at these frequencies. Note that in several instances, the SD best fit to one or more peaks in the amplitude histogram is less than the expected background noise. This point will be taken up again in the Discussion.

EXPERIMENTAL INVESTIGATIONS

We are specifically interested in the contributions of synaptic noise to intracellular voltage recordings in the in vitro rat hippocampal slice. The aim of the following experiments was simply: 1) to determine the contribution of synaptic noise to the recording noise in this preparation; 2) to investigate whether some fraction of this synaptic noise is dependent on the evoked event amplitude; 3) to provide rough estimates of the spontaneous synaptic event frequencies in our recordings.

Methods

The experimental protocols described here follow those described by Larkman et al. (1991). Four- to six-week-old rats (Sprague-Dawley, 120–

TABLE 3 Positions and SD of peaks in amplitude histograms with noise from the stimulated release sites

	Peak 0	Peak 1	Peak 2	Peak 3	Noise SD (q)
(A) Frequency (30-ms refractory period)					
0 Hz					
Mean (q)	0.00	1.00	2.00	3.00	
SD (q)	0.100	0.100	0.100	0.100	0.100
10 Hz					
Mean (q)	−0.04	0.96	1.97	2.98	
SD (q)	0.126	0.129	0.116	0.105	0.122
25 Hz					
Mean (q)	−0.13	0.91	1.94	2.97	
SD (q)	0.214	0.162	0.134	0.113	0.164
50 Hz					
Mean (q)	−0.32	0.76	1.84	2.92	
SD (q)	0.289	0.213	0.178	0.128	0.234
(B) Refractory period (25-Hz frequency)					
0 ms					
Mean (q)	−0.05	0.95	1.95	2.94	
SD (q)	0.229	0.204	0.201	0.202	0.164
15 ms					
Mean (q)	−0.13	0.87	1.89	2.92	
SD (q)	0.195	0.180	0.162	0.143	0.164
30 ms					
Mean (q)	−0.13	0.91	1.94	2.97	
SD (q)	0.214	0.162	0.134	0.113	0.164
60 ms					
Mean (q)	−0.42	0.76	1.88	2.99	
SD (q)	0.301	0.224	0.184	0.101	0.164

160 g) were anesthetized with halothane vapor (Fluothane, ICI) and decapitated. The brain was removed, and 400-μm-thick transverse slices of the hippocampus were cut with a vibrating microtome (Vibroslice, Campden Instruments). During this procedure (3–5 min), the brain was submerged in artificial cerebrospinal fluid (ACSF) at ~2°C. Half of the slices were trimmed to remove area CA3. Trimmed slices were then placed on a lens tissue strip, which was supported by a nylon net in an atmosphere of humidified gas (95% O_2/5% CO_2) in either an interface holding chamber or an interface recording chamber, both at 34–37°C. Slices in both chambers were perfused by ACSF flowing across the lens tissue strip at ~0.1 ml/min. Slices in the recording chamber were left for at least 1 h before recording.

The composition of the ACSF was (in mM) 124 NaCl, 2.3 KCl, 1.26 NaH_2PO_4, 4.0 $MgSO_4$, 4.0 $CaCl_2$, 26 $NaHCO_3$, 10 glucose. Picrotoxin (PTX) (100 μM) and CGP55845A (500 nM) were added to block $GABA_A$ and $GABA_B$ receptor-mediated currents, respectively, and 50 μM D-2-amino-5-phosphonovaleric acid (APV) was added to block NMDA receptor-mediated currents.

Conventional intracellular recordings were made using micropipettes of 25–90 MΩ DC resistance, filled with 2 M potassium methylsulfate. The DC resistance of the electrodes was determined by periodically checking the bridge balance throughout the experimental protocol. Impalements were attempted in the stratum pyramidale of the CA1 region of hippocampus. Signals were amplified wtih an AxoProbe 1A or AxoClamp 2A amplifier, filtered at 2 kHz, and digitized at 5 kHz with a CED 1401 laboratory interface connected to an IBM-PC. Membrane potentials were held at less than −60 mV, using applied steady current via the microelectrode if necessary; currents of no more than 0.7 nA (usually 0.1 or 0.2 nA) were used for this purpose.

Small (less than 2.0 mV) excitatory postsynaptic potentials (EPSPs) were evoked by using extracellular stimulation via a bipolar wire electrode. Note that a minimal stimulation protocol was not used, and therefore more than one axonal fiber might have been stimulated. The stimulating electrode was placed at various positions in the region of the apical dendrites (stratum radiatum) of CA1 pyramidal cells, where Schaffer collateral axons might be stimulated.

After a cell was impaled and it was determined that an EPSP could be evoked, the stimulus was turned off, and 1 s of the voltage time course (the background noise) was recorded. One hundred of such 1-s "sweeps" of data were then recorded sequentially; because of practical limits on the speed of data collection, a 20-ms interval of unrecorded data was interposed between recorded sweeps.

After this measure of the background noise, an EPSP was evoked once every second (1 Hz). One hundred sweeps of 1-s duration were recorded as described above; the EPSP was evoked 0.5 s into each sweep. Tetrodotoxin (TTX) (1 μM) was then washed onto the slice (via the perfusing ACSF); when it was judged that the TTX had reached the slice, 100 sweeps of 1-s duration were again recorded. The TTX continued to perfuse the slice for 5 min, after which a further 100 sweeps were obtained. 6-Cyano-7-nitroquinoxaline-2,3-dione (CNQX) (100 μM) was then added to the perfusing ACSF. Again, when the CNQX reached the slice, 100 sweeps of 1-s duration were recorded, and a further 100 sweeps were recorded 5 min later. During the perfusion of TTX and CNQX, the interval of unrecorded data between recorded sweeps was lengthened to 1 or 2 s, such that changes in the background noise that occurred over several minutes could be observed.

At the end of this protocol, any applied holding current was turned off, and the electrode was removed from the cell (but not from the slice) by moving the electrode upward in 2-μm increments until the measured potential returned to ~0 mV. The background extracellular noise was then recorded in 100 sweeps of 1 s duration, with an intersweep interval of 20 ms.

Data analysis

The average time course of the evoked EPSP in each cell was obtained by averaging the EPSPs recorded before the addition of TTX. A 2.5-ms window was positioned immediately before the stimulus artefact, and a second 2.5-ms window was positioned by eye at the peak of the average EPSP (see Fig. 1 *A*). Subtracting the mean amplitude of the first window from the second gives a measure of the amplitude of the average EPSP. The positions of these windows, determined on the average EPSP, could also be used to measure the amplitude of each EPSP evoked in that cell.

For each set of 100 sweeps, noise amplitudes were measured by subtracting the amplitudes of two 2.5-ms windows, spaced at the distance determined from the average EPSP for that cell, but positioned away from the evoked event. Between 10 and 50 nonoverlapping measures were made on each sweep before the applied stimulus. This gave 1000–5000 noise measures from which the variance of the background noise could be calculated.

Data analysis and simulations were written in C and performed on a SUN workstation. Best fits were obtained via the Nelder-Mead downhill simplex algorithm "amoeba" (Press et al., 1988). The standard deviation of best-fit parameters was calculated from the system covariance matrix (Landaw and DiStephano, 1984). Unless otherwise noted, the statistical significance between measures obtained under different recording conditions has been judged at the 95% level, using a one-tailed Wilcoxon signed rank test for paired data. Numerical values are reported as mean ± SD unless noted.

RESULTS

The experimental protocol was completed in 10 neurons. The variance of the background noise recorded outside of the cell varied between 1225 and 8650 μV^2, showing some correlation with variations in the DC resistance of the microelectrode (correlation coefficient, $r = 0.28$; data not shown). To correct for these differences, the variance of this noise was subtracted from the variance of the noise measured during other conditions in the same cell; this result is referred to in the following sections as the corrected noise variance. If the electrode resistance changed by 10 MΩ or more during the course of the protocol, data from that cell were excluded from the analysis (one of 10 cells). No significant differences in intracellular noise levels were observed between hippocampal slices in which area CA3 was left intact or trimmed from the slice, and data from all hippocampal slices were pooled for analysis on this basis. We also examined changes in noise variance with time for each cell during the ~10-min interval before drugs were applied and saw no systematic changes; although in a few cells the noise increased gradually over time, in others it decreased and there were no significant trends on average.

Fig. 7 *A* shows one example of a smoothed histogram of the noise amplitudes measured in a hippocampal pyramidal cell at the beginning of a wash-in experiment, after TTX wash-in, and after CNQX wash-in. As demonstrated in the figure, noise amplitude distributions were generally unimodal, with a mean that was close to zero and no visible skewness.

Contributions of synaptic noise

Fig. 7 *B* shows the effect on the corrected noise variance of washing TTX and CNQX onto the slice (average values for nine neurons). The first time point shows the corrected noise variance obtained before stimulating the EPSP; the second

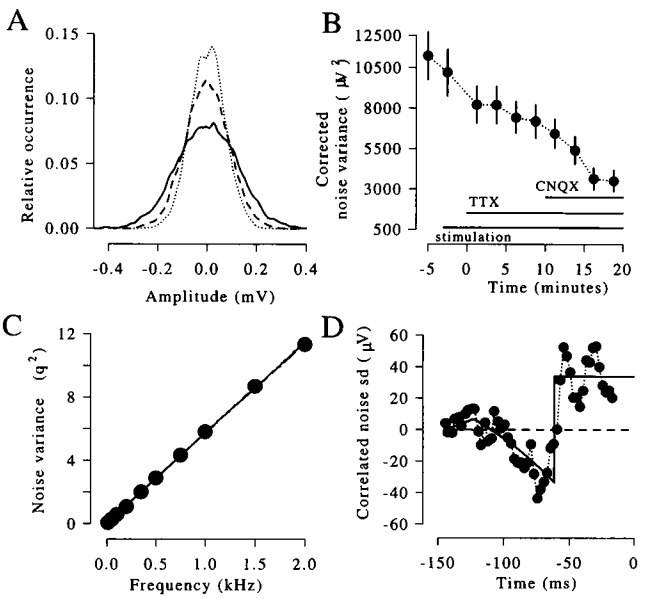

FIGURE 7 (*A*) Examples of the noise amplitude distributions recorded in a CA1 hippocampal pyramidal neuron. For each distribution shown, 5000 noise amplitudes were measured as described in the text; each distribution was smoothed by a digital Gaussian filter with a SD of 10 μV to help visualize the overall shape. The distributions of noise amplitudes recorded before the EPSP was evoked (——), after TTX wash-in (– – –), and after CNQX wash-in (·····) are shown. In all three cases the noise distributions are roughly symmetrical and centered at zero. Note the decrease in the noise variance after both TTX and CNQX wash-in. (*B*) Effects of TTX and CNQX wash-in. Noise variance has been corrected for background noise recorded outside the cell and plotted against time for nine CA1 hippocampal pyramidal cells (●···●). Mean values ± SEM are shown. The first time point shows the variance of the noise recorded before extracellular stimulation was applied to evoke a small EPSP. TTX was washed onto the slice from time 0 to 20 min, CNQX from time 10 to 20 min. Consecutive 1-s traces recorded at 0.33 Hz during wash-in were separated into groups of 50 for analysis. (*C*) Simulated noise variance as a function of spontaneous event frequency. Simulated data were produced in which spontaneous single quantal events, modeled by a double-exponential EPSP waveform (Fig. 1 *A*) and scaled to unit amplitude, occurred at specified frequencies. Five thousand noise amplitudes were measured for each frequency, as described in the text. The standard deviation of the noise is plotted against frequency (●) and describes a smooth curve. A linear regression was performed on these data; the best fit is plotted (——) and is given by Eq. 11. (*D*) Correlated noise. The correlated noise SD measured at times before the applied stimulus is plotted against time for nine CA1 pyramidal cells (●···●). The best fit of the probability function $p_c(t)$ to these data is shown by the solid line; $p_c(t)$ has been scaled by a constant that is a free parameter of the fit (the *y*-intercept). Although the measured data are quite noisy, the analytical prediction appears to describe the observed behavior well.

shows the noise recorded during the recording of the EPSP. The noise appears to drop between these two conditions; however, this difference is not significant. Noise levels decrease during TTX wash-in; the difference between the noise variance recorded before stimulating and the noise variance 7.5 min after TTX wash-in was significant at the 99% level. Note also the marked decrease in the noise variance 7.5 min after the wash-in of CNQX (significant at the 99.5% level).

Table 4 shows the variances of the various components of the noise isolated in this procedure (n = 9). Values in the left column show the uncorrected noise variance recorded at various points in the protocol. The prestimulus noise is the noise variance recorded intracellularly at the beginning of the experiment, which is slightly (and not significantly) greater than the noise measured while the EPSP was being evoked. The noise recorded "after TTX" or "after CNQX" corresponds to the last time point during the wash-in period, as shown in Fig. 7 *B*. The noise recorded outside the cell consists largely of noise from the microelectrode and recording apparatus, and accounted for ~30% of the total noise variance.

Values in the second column show the average noise variance obtained after values in each cell were corrected for background noise recorded outside the cell. Values in the third and fourth numerical columns show the isolated contributions of various noise components and their percentage contributions to the total intracellular noise. The TTX-sensitive and CNQX-sensitive (TTX-insensitive) components of the noise account for, respectively, ~30% and 35% of the intracellular noise variance.

Simulations of spontaneous events at different frequencies

Table 4 illustrates that synaptic noise accounts for ~65% of the total noise recorded intracellularly under the conditions used in these experiments. To shed some light on what frequencies of spontaneous events would be necessary to obtain this result, a simulation was performed in which spontaneous single quantal events were generated at a given frequency. The timing of the events was Poisson distributed; the shape of the event was modeled after an average EPSP recorded in one cell (Fig. 1 *A*), scaled to unit amplitude.

Simulated traces 1 s long were subjected to the same analysis of the background noise as was used for the experimental data. Fig. 7 *C* plots the resulting noise variance against simulated event frequency. The solid line in the figure shows the results of a least-squares linear regression, and is given by

$$F = 0.174 v_p \qquad (11)$$

where F is the frequency of the spontaneous events, in kHz, and v_p is the predicted variance of the noise. The form of this equation may be generally applicable in experimental situations where the majority of spontaneous synaptic events are monoquantal and event superposition is roughly linear, but the slope of the regression will depend on the average shape of the single quantal event at the recording site. Also note that under the assumptions of this model, the synaptic noise SD will scale linearly with quantal size (see Clamann et al., 1991).

Equation 11 may be used to predict the spontaneous event frequency, given the measured noise variance. The CNQX-sensitive (TTX-insensitive) component of the noise in our

TABLE 4 Contributions of various components of the recording noise

	Noise variance (μV^2)	Corrected variance (μV^2)	Noise contribution	Variance (μV^2)	Percentage of "total" noise
Prestimulus	14640 ± 440	11500 ± 440			
During EPSP	13690 ± 440	10550 ± 440	Intracellular	10550 ± 440	100%
After TTX	10680 ± 320	7540 ± 320	TTX-sensitive	3010 ± 540	28.5 ± 5.1%
After CNQX	6830 ± 320	3690 ± 320	CNQX-sensitive*	3850 ± 450	36.5 ± 4.3%
Outside cell	3140 ± 40	∅	CNQX-insensitive	3690 ± 320	35.0 ± 3.0%

*TTX-insensitive.

preparation had a corrected variance of 3850 ± 450 μV^2 (Table 4). If we assume a quantal amplitude, as recorded at the soma, of 150 μV (Larkman et al., 1991; Voronin et al., 1992a), this corresponds to a noise variance of 0.11–0.22 squared quantal amplitudes (confidence limits corresponding to ±2 SD). From Eq. 11, the frequency of spontaneous synaptic events predicted by the model is then 20–38 Hz (mean 29 Hz).

This estimate assumes that TTX-insensitive, CNQX-sensitive noise consists entirely of single quantal synaptic events, and therefore provides upper limits on the spontaneous event frequency. Although this method is clearly less accurate and elegant than event-counting algorithms used elsewhere (eg. Korn and Faber 1990), it has the advantage of being applicable to recordings with very high background noise levels or high spontaneous event frequencies, in which individual miniature events are often obscured.

Correlated noise

The EPSPs evoked before TTX wash-in provide data with which it is possible to address the important issue of correlations between evoked EPSP amplitudes and the background noise. We divided EPSP sweeps from each cell into three equal membership groups on the basis of amplitude, and then compared the noise immediately preceding the group of "small" EPSPs with the noise preceding the "large" events as described below. Because we wish to compare this result with the predicted probabilities of spontaneous event occurrence, synaptic noise SD, as opposed to variance, has been used throughout this section.

For each sweep, the background noise from immediately before to 150 ms before the stimulus was determined by shifting both measurement windows (shown in Fig. 1 *A*) backward in time in 2.5-ms increments (the width of one window). The average recorded value in the first window was subtracted from that in the second to produce a noise amplitude. All of the "small" sweeps from one cell were identified, and the noise amplitudes for each 2.5-ms time interval in the ensemble of sweeps were pooled. To get an estimate of the SD of the noise, noise amplitudes for each 2.5-ms interval and for two intervals (5 ms) before and after each time point were included, which effectively produced a moving average of noise SD. To isolate the component of the noise that is correlated with EPSP amplitude, the SD of the noise before the "large" evoked EPSPs from each cell was subtracted from the SD of the noise before "small" events. We use the term "correlated noise" to describe this result.

If the correlated noise is positive, it implies that the noise before small events is generally greater than the noise before large EPSPs—or effectively, that if noise levels are high at this time preceding the stimulus, a large evoked EPSP is unlikely. Conversely, if the correlated noise is negative, an evoked EPSP is more likely to be large if noise levels are high at this time point. Zero correlated noise implies that the amplitude of the evoked EPSP is independent of the noise at this time.

The circles in Fig. 7 *D* illustrate the correlated noise versus time for pooled data from nine hippocampal pyramidal cells. Note that in this figure time is plotted in milliseconds before the applied stimulus, which occurs at time 0, on the right-hand edge of the graph. These data suggest that high noise levels from zero to 50–60 ms before the applied stimulus decrease the probability of recording a large evoked EPSP, whereas high noise levels 60–100 ms before the stimulus increase the probability that the EPSP amplitude is large. The average correlated noise in the 50 ms immediately preceding the stimulus is 32.0 ± 0.9 μV^2, which corresponds to 10% of the intracellular noise for these cells.

Model fitting

The similarities between the analytical prediction for correlated noise (Fig. 5) and the experimental data shown for hippocampal neurons in Fig. 7 *D* are striking. Although one would ideally like to fit the complete analytical model (derived in the Appendix) to the experimental data, the data illustrated in Fig. 7 *D* are too noisy to merit such an approach. As shown in Fig. 8, the predicted correlated noise standard deviation, $SD_c(t)$, provides a good (although scaled) estimate of the measured SD of the correlated noise, and relies on a relatively small number of parameters.

The free variables of such a fit are the length of the refractory period, R (in ms), the spontaneous event probability for nonrefractory sites, f, and the variance offset (effectively the y-intercept of the function shown in Fig. 7 *D*) (in μV^2). Fig. 7 *D* shows the best-fit curve against the measured data for correlated noise in hippocampal CA1 pyramidal cells. For this fit, the model predicts a refractory period of 61.4 ± 0.7 ms, a probability f of 0.0099 ± 0.0068

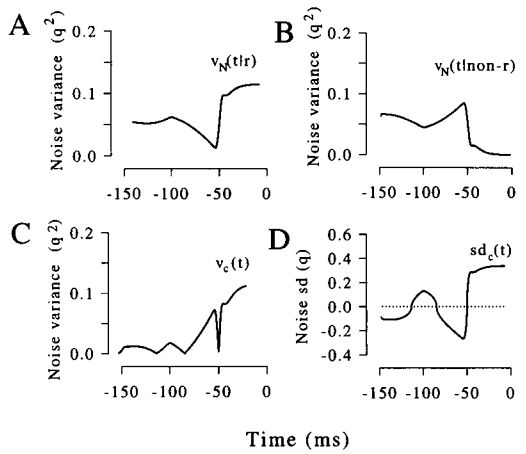

FIGURE 8 Analytical model of correlated noise SD. Solutions to the equations describing the SD of the correlated noise are presented for a model with a refractory period, R, of 50 ms, and a probability of spontaneous events, f, of 16.67 s^{-1}. The variance (in squared quantal units) of the noise from the stimulated site at time t, given that the site is refractory (A) or nonrefractory (B) at zero, is shown. The difference between these curves, the predicted variance of the correlated noise, is shown in C. To compare these results to the predicted probability of spontaneous events (Fig. 5), SD, as opposed to variance, must be used; the square root of the curve shown in B has been subtracted from the square root of the curve in C, and the result, the correlated noise SD, is shown in D. Note the similarity between the shape of this curve and the correlated noise probability in Fig. 5 C.

in each ms, and a y-intercept of 34.0 ± 23.4 μV^2 (each parameter reported as best-fit value ± SD from the covariance matrix of the least-squares fit). The small SD of the predicted refractory period reveals a very high sensitivity of the fit to this parameter; the model predicts that the stimulated sites have a refractory period of between 60.0 and 62.8 ms (±2 SD).

Although the model is clearly much less sensitive to predictions for the spontaneous event rate or the y-intercept, some interesting calculations can be made based on the best-fit values of these parameters. As discussed previously, the rate of spontaneous events during the segment of the curve immediately preceding the stimulus is expected to be $1/R$ (16.3 Hz). Equation 11 predicts that this frequency of spontaneous events would cause a noise variance of 0.0937 squared quantal units, therefore: 1156 $\mu V^2 = 0.0937q^2$, and q, the single quantal amplitude, is predicted to be 111 μV. This prediction overestimates q if, on average, the difference in the number of release sites contributing to "small" versus "large" events is greater than one. The extent of this overestimation will increase (sublinearly) with this difference, but decrease if the probability of response to the applied stimulus, p, is less than 1.

The model predicts that spontaneous events from the stimulated sites occur with a probability, during each millisecond when the site is nonrefractory, of ~0.01. Thus each site spends, on average, 0.1 s in the nonrefractory state before firing, followed by 0.06 s in the refractory state. This corresponds to a frequency of spontaneous firing from the stimulated sites of ~6 Hz, whereas the total frequency of spontaneous events is estimated (see Fig. 7 C) to be ~30 Hz. Thus spontaneous events from the stimulated sites may account for 10–20% of the spontaneous events recorded in hippocampal CA1 cells under these conditions.

DISCUSSION

The effects of synaptic noise on amplitude histograms

The simple experiments outlined above indicate that the contribution of synaptic noise to the overall background noise in our recordings can be substantial, and that a component of this synaptic noise is correlated with the evoked EPSP amplitude. We also find that histograms recorded in this and in similar preparations show qualities that are consistent with our analytical models of histograms recorded in high levels of synaptic noise. It is important to note that these analytical models are not presented with a view to including synaptic noise as an additional variable in model fits to evoked amplitude histograms.

Specifically, our models predict that background synaptic noise at frequencies of 25 Hz or higher (Table 2) or synaptic noise from the stimulated release sites (Table 3) can cause the SD of peaks on the right of the histogram to be less than the SD of peaks on the left—"apparent negative quantal variance." This is probably due in part to the effect of fitting Gaussian curves to peaks that are negatively skewed, and in part to noise-contaminated events from higher peaks being attributed to lower peaks in the histogram—some of the variance of the higher peaks is effectively "passed down" to neighboring peaks on the left. We have previously observed apparent negative quantal variance in 17 of 22 synaptic amplitude histograms recorded in CA1 pyramidal cells (Stratford et al., 1994). The effects of intersite differences in quantal size could also contribute to this phenomenon for synaptic contacts with a high overall release probability (Wahl et al., 1995).

Synaptic noise from the stimulated sites may also contribute less noise during the evoked event than during a comparable baseline period, particularly on the right-hand side of the histogram (see Table 3 and Fig. 6). This "noise reduction" may be due in part to amplitudes at the extremes of the noise distribution; in a multimodal histogram, these outliers will be "attributed" by the fitting procedure to neighboring peaks, minimizing the variance of the best-fit Gaussian distributions. Another factor in this effect, however, may be the nonindependence of signal and noise imposed by a period of refractoriness after release. This phenomenon has been observed in several studies of synaptic amplitude histograms recorded in hippocampus (Larkman et al., 1991; Liao et al., 1992; Voronin et al., 1992a; Stricker et al., 1996a); other possible mechanisms are the effects of both data selection and finite sampling.

Fig. 6 illustrates that synaptic noise from the stimulated sites may change the relative heights and areas of the peaks

in the evoked amplitude histogram. This effect is, of course, due to the higher probability that a given release site is in a refractory state at the time of the stimulus—the probability that a release site will fire in response to the stimulus has in fact been reduced. The frequency of synaptic noise from the stimulated sites may therefore be a significant factor in determining the release probability for a given connection, and release probabilities may vary in a use-dependent manner.

The amplitude distribution of synaptic noise

The simulations and analytical modeling presented in this paper illustrate the complex effects of synaptic background noise on the measured amplitudes of synaptic events. Synaptic noise distributions generally exhibit one or more subpeaks to the left of the origin, caused by the higher probability of making a measurement during the falling phase, rather than the rising phase, of a spontaneous event. Although these subpeaks will not be individually discernible if even very small amounts of additional Gaussian noise are present in the recording, their combined effect can be observed, even at low event frequencies. As seen in Figs. 2 and 3, the central peak of the synaptic noise distribution is shifted to the left of the origin and is slightly skewed to the left.

Noise distributions recorded intracellularly in hippocampal pyramidal cells, however, are often either well approximated by a single Gaussian function or positively skewed (Kullmann, 1989; Sayer et al., 1989, 1990; Larkman et al., 1991; Voronin et al., 1992a; Stricker et al., 1994, 1996a). Because TTX was not used in any of the above studies, however, multiquantal spontaneous events could be responsible for this effect. Although inhibitory synaptic noise might also contribute to positively skewed noise distributions, synaptic inhibition was blocked pharmacologically in most of these experiments (Kullmann, 1989; Sayer et al., 1989, 1990; Larkman et al., 1991; Stricker et al., 1994, 1996a).

The frequency of spontaneous miniature events

The mean frequency of spontaneous miniature events in hippocampal pyramidal cells, at room temperature and in the absence of TTX, has been estimated to be 1.0 or 1.7 Hz (Manabe et al., 1992; McBain and Dingledine, 1992; respectively). Neither of these studies reported a significant decrease in this rate with the addition of TTX to the bathing media, which is in contrast to results in the goldfish Mauthner cell (Korn and Faber, 1990; Korn et al., 1993) and the kitten spinal motoneuron (Hubbard et al., 1967). In hippocampal neurons in the presence of TTX, other estimates of this frequency range from 0.8 to 1.0 Hz (Finch et al., 1990; Manabe et al., 1992; McBain and Dingledine, 1992).

Several studies, however, have illustrated the profound sensitivity of this rate to variations in the recording conditions or protocol. Manabe et al. (1992) reported a doubling of the rate of spontaneous miniature events in CA1 pyramidal cells while stimulating Schaffer collateral axons at 0.2 Hz; this increase was brought back to baseline by TTX, indicating that stimulation of afferent axons can greatly increase the frequency of spontaneous events. In studies of paired-pulse modulation performed in microcultures of rat hippocampus, Mennerick and Zorumski (1995) report average spontaneous event frequencies of 30–40 Hz immediately after an evoked event; this frequency returned to baseline (1 or 2 Hz) within ~1 s after the evoked EPSC. Raastad et al. (1992) report that miniature events are rare in cultured hippocampal neurons bathed in 2 mM external calcium, but that in 1 mM calcium, spontaneous events are much more frequent, and are highly sensitive to TTX. Finch et al. (1990) report a spontaneous event rate of 0.81 Hz at 22°C, which rises to 15.8 Hz at 34–37°C, also in cultured hippocampal neurons.

The experimental data summarized in Fig. 7 were recorded by sharp microelectrodes at 34–37°C, with 4 mM external calcium concentration, and with stimulation at modest frequencies (1 Hz). Our results suggest that under these conditions, ~65% of the intracellular recording noise is synaptic in origin, over half of which is due to action potential-independent release of neurotransmitter at frequencies with a predicted upper limit of ~30 Hz.

Correlated noise

The analysis of correlated noise in hippocampal pyramidal cells suggests that up to 20% of the synaptic noise immediately before the stimulus is correlated with evoked EPSP amplitude. Korn and his collegues (Korn and Faber, 1990; Korn et al., 1993) found evidence that the synaptic noise recorded at a central inhibitory synapse arises from high-frequency bursts of firing from a small subset of available synapses. As discussed earlier, the frequency of miniature EPSCs has been found to increase during or immediately after evoking synaptic events (Manabe et al., 1992; Mennerick and Zorumski, 1995). Thus it seems likely that many of the spontaneous events recorded during stimulation may be promoted by action potentials in the stimulated fibers, and therefore occur at the same sites that produce the evoked event, although release sites in a network of cells that have been indirectly "wound up" by the stimulation could also contribute. As discussed above for background synaptic noise, we expect that this estimate of 20% correlated noise is highly sensitive to variations in recording conditions and protocol.

The behavior of the correlated noise component is consistent with a model which assumes that each release site experiences a refractory period—a time interval during which release probability drops to near zero—after initiating a spontaneous event. The refractory period for a single release site predicted by our model is 60 ms. This is in good agreement with the results of Stevens and Tsujimoto (1995), who report release rates in cultured hippocampal neurons

that peak at 14 quanta per bouton per second, or 71 ms between subsequent events at a single bouton (but see Stevens and Wang, 1995). In studies of transmitter release at retinal amacrine cells, Borges et al. (1995) report a peak release rate of 150 quanta per release site per second, which corresponds to a 6-ms interval between subsequent events. This high frequency cannot be maintained, however, and the release rate reaches a plateau at 22 quanta per site per second, or 45 ms between events.

The refractory period could represent the time required to reload the release site—to dock or prime filled synaptic vesicles, or to refill a vesicle that stays in place. If the noise that is correlated with evoked EPSP amplitude is in some sense related to spontaneous action potentials, then a refractoriness of the stimulated fiber or of individual release sites would explain our results. Finally, it is important to note that refractoriness need not be an all-or-nothing change of state, as modeled here for simplicity. Depending on the exact mechanism(s) of refractoriness, the probability of releasing a quantum may drop to near zero and recover gradually over a period of time, as has been suggested experimentally at these synapses (for example, Stevens and Wang, 1995).

APPENDIX: PREDICTED NOISE VARIANCE

Having derived the probability of occurrence of a spontaneous event as a function of time, given the state of the release site at the stimulus, we will determine how this probability relates to the predicted variance of the noise. The noise variance at any time t, $v_N(t)$, contains contributions from events occurring at that time, and from all of the events initiated at previous times that have not yet decayed to zero. Consider the EPSP waveform illustrated in Fig. 1 *A*, and the two 2.5-ms windows used to measure amplitude as shown. The third panel of the figure illustrates the difference function, $d(s)$, obtained if both windows are shifted forward by time s and the amplitude measured. This function illustrates the noise amplitude that would be recorded if a spontaneous event were to occur at some time $t - s$ before the time of the noise measurement, t.

Fig. 7 *C* illustrates the predicted noise variance as a function of spontaneous event frequency, for a unit quantal size. If the frequency of spontaneous events is a given value at t (the time of the noise measurement) and at all times previous to t, this figure (or Eq. 11) can be used to predict $v_N(t)$. If the spontaneous event frequency is not constant, however, then a weighted average of previous variance values is necessary.

The weights for this average are provided by the difference function, shown in Fig. 1 *B*. This function shows the contribution to the noise variance measured at t that is made by events occurring at some previous time, $t - s$. Once the spontaneous event frequency at $t - s$ is known, the predicted noise variance for this previous time, $v_p(t - s)$, can be obtained from Eq. 11. Because variances add linearly, we weight this value by $w(s)$, the square of the difference function at s. If these weighted variance values are integrated for all times before t and the result is divided by the integral of the weighting function, an estimated value for the variance measured at t is obtained:

$$v_N(t) = \frac{\int_{s=0}^{\infty} v_p(t - s)w(s)\delta s}{\int_{s=0}^{\infty} w(s)\delta s} \qquad (A.1)$$

In practice, it is fair to assume that an event initiated at zero will effectively decay to zero amplitude by time T ($w(s) = 0$ for $s > T$), and the integration limits will therefore not extend to infinity.

The application of Eq. A.1 to $p(t|r)$ and $p(t|\text{non-}r)$ as derived above is shown in Fig. 8, *A* and *B*. These curves represent the predicted noise variance attributable to spontaneous events occurring before the stimulus, given the state of the release site (refractory or nonrefractory) at the stimulus.

If any release site is refractory at the time of the stimulus, a smaller EPSP is likely to be evoked. The final step in this analytical model is to subtract the noise variance predicted for nonrefractory release sites from that predicted for refractory release sites to obtain the correlated noise, $v_c(t)$, as shown in Fig. 8 *C*. For comparison to the noise probability function, we must consider the SD, as opposed to the variance, of the noise. To illustrate this comparison, the square root of $v_N(t|\text{non-}r)$ has been subtracted from the square root of $v_N(t|r)$, and the result is plotted in Fig.8 *D* ($SD_c(t)$). Note the similarity between the shape of this function and that illustrated in Fig. 5 *C*.

We thank Dr. M. E. Barish for suggesting helpful references and Dr. M. A. Nowak for comments on the mathematics.

This work was supported by the Natural Sciences and Engineering Research Council of Canada, by the Wellcome Trust, and by EPSRC grant GR/J/24812.

REFERENCES

Auerbach, A. A. 1971. Spontaneous and evoked quantal transmitter release at a vertebrate central synapse. *Nature New Biol.* 234:181–183.

Barrett, E. F., J. N. Barrett, A. R. Martin, and R. Rahamimoff. 1974. A note on the interaction of spontaneous and evoked release at the frog neuromuscular junction. *J. Physiol. (Lond.).* 237:453–463.

Bekkers, J. M., G. B. Richerson, and C. F. Stevens. 1990. Origin of variability in quantal size in cultured hippocampal neurons and hippocampal slices. *Proc. Natl. Acad. Sci. USA.* 87:5359–5362.

Bekkers, J. M., and C. F. Stevens. 1990. Presynaptic mechanism for long-term potentiation in the hippocampus. *Nature.* 346:724–729.

Bekkers, J. M., and C. F. Stevens. 1995. Quantal analysis of EPSCs recorded from small numbers of synapses in hippocampal cultures. *J. Neurophysiol.* 73:1145–1156.

Blum, K. I., and M. A. P. Idiart. 1994. A theoretical framework for quantal analysis and its application to long-term potentiation. *J. Neurophysiol.* 72:1395–1401.

Borges, S., E. Gleason, M. Turelli, and M. Wilson. 1995. The kinetics of quantal transmitter release from retinal amacrine cells. *Proc. Natl. Acad. Sci. USA.* 92:6896–6900.

Bornstein, J. C. 1978. Spontaneous multiquantal release at synapses in guinea-pig hypogastric ganglia: evidence that release can occur in bursts. *J. Physiol. (Lond.).* 282:375–398.

Boyd, I. A., and A. R. Martin. 1956. The end-plate potential in mammalian muscle. *J. Physiol. (Lond.).* 132:74–91.

Brown, T. H., R. K. S. Wong, and D. A. Prince. 1979. Spontaneous miniature synaptic potentials in hippocampal neurons. *Brain Res.* 177: 194–199.

Clamann, H. P., M.-S. Rioult-Pedotti, and H.-R. Lüscher. 1991. The influence of noise on quantal EPSP size obtained by deconvolution in spinal motoneurons in the cat. *J. Neurophysiol.* 65:67–75.

Cohen, I., H. Kita, and W. Van der Kloot. 1974. The intervals between miniature end-plate potentials in the frog are unlikely to be independently or exponentially distributed. *J. Physiol. (Lond.).* 236:327–339.

del Castillo, J., and B. Katz. 1954. Quantal components of the end-plate potential. *J. Physiol. (Lond.).* 124:560–573.

Dityatev, A. E., V. M. Kozhanov, and S. O. Gapanovich. 1992. Modelling of the quantal release at interneuronal synapses: analysis of permissible values of model moments. *J. Neurosci. Methods.* 43:201–214.

Edwards, F. R., S. J. Redman, and B. Walmsley. 1976. Statistical fluctuations in charge transfer at Ia synapses on spinal motoneurones. *J. Physiol. (Lond.).* 259:665–688.

Finch, D. M., R. S. Fisher, and M. B. Jackson. 1990. Miniature excitatory synaptic currents in cultured hippocampal neurons. *Brain Res.* 518: 257–268.

Foster, T. C., and B. L. McNaughton. 1991. Long-term enhancement of CA1 synaptic transmission is due to increased quantal size, not quantal content. *Hippocampus.* 1:79–91.

Hubbard, J. I., D. Stenhouse, and R. M. Eccles. 1967. Origin of synaptic noise. *Science.* 157:330–331.

Jack, J. J. B., S. J. Redman, and K. Wong. 1981. The components of synaptic potentials evoked in cat spinal motoneurones by impulses in single group Ia afferents. *J. Physiol. (Lond.).* 321:65–96.

Katz, B., and R. Miledi. 1965. The effect of temperature on the synaptic delay at the neuromuscular junction. *J. Physiol. (Lond.).* 181:656–670.

Korn, H., F. Bausela, S. Charpier, and D. Faber. 1993. Synaptic noise and multiquantal release at dendritic synapses. *J. Neurophysiol.* 70: 1249–1254.

Korn, H., and D. S. Faber. 1987. Regulation and significance of probabilistic release at central synapses. *In* Synaptic Function. G. M. Edelman, W. E. Gall, and W. M. Cowan, editors. Wiley, New York. 57–108.

Korn, H., and D. S. Faber. 1990. Transmission at a central inhibitory synapse. IV. Quantal structure of synaptic noise. *J. Neurophysiol.* 63: 198–222.

Korn, H., and D. S. Faber. 1991. Quantal analysis and synaptic efficacy in the CNS. *Trends Neurosci.* 14:439–445.

Kullmann, D. M. 1989. Applications of the expectation-maximization algorithm to quantal analysis of postsynaptic potentials. *J. Neurosci. Methods.* 30:231–245.

Kullmann, D. M. 1992. Quantal analysis using maximum entropy noise deconvolution. *J. Neurosci. Methods.* 44:47–57.

Kullman, D. 1993. Quantal variability of excitatory transmission in the hippocampus: implications for the opening probability of fast glutamate-gated channels. *Proc. R. Soc. Lond. Biol.* 253:107–116.

Kullmann, D. M., and R. A. Nicoll. 1992. Long-term potentiation is associated with increases in both quantal content and quantal amplitude. *Nature.* 357:240–244.

Kuno, M. 1964. Quantal components of excitatory synaptic potentials in spinal motoneurones. *J. Physiol. (Lond.).* 175:81–99.

Landaw, E. M., and J. J. DiStephano, III. 1984. Multi-exponential, multi-compartmental, and non-compartmental modelling. II. Data analysis and statistical considerations. *Am. J. Physiol.* 246:R665–R677.

Larkman, A., T. Hannay, K. Stratford, and J. Jack. 1992. Presynaptic release probability influences the locus of long-term potentiation. *Nature.* 360:70–73.

Larkman, A., K. Stratford, and J. Jack. 1991. Quantal analysis of excitatory synaptic action and depression in hippocampal slices. *Nature.* 350: 344–347.

Liao, D., A. Jones, and R. Malinow. 1992. Direct measurement of quantal changes underlying long-term potentiation in CA1 hippocampus. *Neuron.* 9:1089–1097.

Ling, L., and D. J. Tolhurst. 1983. Recovering the parameters of a finite mixture of normal distributions from a noisy record: an empirical comparison of different estimating procedures. *J. Neurosci. Methods.* 8:309–333.

Malinow, R. 1991. Transmission between pairs of hippocampal slice neurones: quantal levels, oscillations, and LTP. *Science.* 252:722–724.

Malinow, R., and R. W. Tsien. 1990. Presynaptic enhancement shown by whole-cell recordings of long-term potentiation in hippocampal slices. *Nature.* 346:177–180.

Manabe, T., P. Renner, and R. A. Nicoll. 1992. Postsynaptic contribution to long-term potentiation revealed by the analysis of miniature synaptic currents. *Nature.* 355:50–55.

McBain, C., and R. Dingledine. 1992. Dual-component miniature excitatory synaptic currents in rat hippocampal CA3 pyramidal neurons. *J. Neurophysiol.* 68:16–27.

Mennerick, S., and C. F. Zorumski. 1995. Paired-pulse modulation of fast excitatory synaptic currents in microcultures of rat hippocampal neurons. *J. Physiol. (Lond.).* 488:85–101.

Papoulis, A. 1991. Probability, Random Variables and Stochastic Processes. McGraw-Hill, New York.

Press, W. H., B. P. Flannery, S. A. Teukolsky, and W. T. Vetterling. 1988. Numerical Recipes: The Art of Scientific Computing. Cambridge University Press, Cambridge.

Raastad, M., J. F. Storm, and P. Andersen. 1992. Putative single quantum and single fibre excitatory postsynaptic currents show similar amplitude range and variability in rat hippocampal slices. *Eur. J. Neurosci.* 4:113–117.

Rahamimoff, R., and Y. Yaari. 1973. Delayed release of transmitter at the frog neuromuscular junction. *J. Physiol. (Lond.).* 228:241–257.

Redman, S. 1990. Quantal analysis of synaptic potentials in neurons of the central nervous system. *Physiol. Rev.* 70:165–198.

Sayer, R. J., M. J. Friedlander, and S. J. Redman. 1990. The time course and amplitude of EPSPs evoked at synapses between pairs of CA3/CA1 neurons in the hippocampal slice. *J. Neurosci.* 10:826–836.

Sayer, R. J., S. J. Redman, and P. Andersen. 1989. Amplitude fluctuations in small EPSPs recorded from CA1 pyramidal cells in the guinea pig hippocampal slice. *J. Neurosci.* 9:840–850.

Solodkin, M., I. Jiménez, W. F. Collins, III, L. M. Mendell, and P. Rudomin. 1991. Interaction of baseline synaptic noise and Ia EPSPs: evidence for appreciable negative correlation under physiological conditions. *J. Neurophysiol.* 65:927–945.

Soucek, B. 1971. Influence of the latency fluctuations and the quantal process of transmitter release on the end-plate potentials' amplitude distribution. *Biophys. J.* 11:127–139.

Stevens, C. F. 1993. Quantal release of neurotransmitter and long-term potentiation. *Cell. (Neuron.* 10)72:55–63.

Stevens, C. F., and T. Tsujimoto. 1995. Estimates for the pool size of releasable quanta at a single central synapse and for the time required to refill the pool. *Proc. Natl. Acad. Sci. USA.* 92:846–849.

Stevens, C. F., and Y. Wang. 1995. Facilitation and depression at a single central synapse. *Neuron.* 14:795–802.

Stratford, K., A. Larkman, and J. Jack. 1994. Apparent negative quantal variance at excitatory synapses in CA1 of rat hippocampal slices in vitro. *J. Physiol. (Lond.).* 176P:69P.

Stricker, C., A. C. Field, and S. J. Redman. 1996a. Statistical analysis of amplitude fluctuations in EPSCs evoked in rat CA1 pyramidal neurones in vitro. *J. Physiol. (Lond.).* 490:419–441.

Stricker, C., A. C. Field, and S. J. Redman. 1996b. Changes in quantal parameters of EPSCs in rat CA1 neurones in vitro after the induction of long-term potentiation. *J. Physiol. (Lond.).* 490:443–454.

Stricker, C., and S. Redman. 1994. Statistical models of synaptic transmission evaluated using the expectation-maximization algorithm. *Biophys. J.* 67:656–670.

Turner, D. A., and M. West. 1993. Bayesian analysis of mixtures applied to postsynaptic potential fluctuations. *J. Neurosci. Methods.* 47:1–21.

Van der Kloot, W., and J. Molgó. 1995. The relationship between quantal content and delayed quantal release. *Neuroreport.* 6:1807–1810.

Voronin, L. L., U. Kuhnt, G. Hess, A. G. Gusev, and V. Roschin. 1992a. Quantal parameters of "minimal" excitatory postsynaptic potentials in guinea pig hippocampal slices: binomial approach. *Exp. Brain Res.* 89:248–264.

Voronin, L. L., U. Kuhnt, G. Hess, A. G. Gusev, and V. Roschin. 1992b. Quantal analysis of long-term potentiation of "minimal" excitatory postsynaptic potentials in guinea pig hippocampal slices: binomial approach. *Exp. Brain Res.* 89:275–287.

Wahl, L. M., K. J. Stratford, A. U. Larkman, and J. J. B. Jack. 1995. The variance of successive peaks in synaptic amplitude histograms: effects of inter-site differences in quantal size. *Proc. R. Soc. Lond. Biol.* 262: 77–85.

Wong, K., and S. Redman. 1980. The recovery of a random variable from a noisy record with application to the study of fluctuations in synaptic potentials. *J. Neurosci. Methods.* 2:389–409.